



Journal of Hunan University (Natural Sciences)

Vol. 52 No. 9
September 2025

Available online at
<https://jonuns.com>



ELSEVIER
Scopus



Clarivate
WEB OF SCIENCE

Open Access Article

 <https://doi.org/10.55463/issn.1674-2974.52.9.15>

Gully Erosion Risk Assessment Using Multi-Criteria Analysis: A Case Study of the Oued Rhéraya Watershed

Aïcha Fadil^{1*}, Farid El Wahidi²

¹Geomorphology, Environment and Society Laboratory, FLSH, UCA, Marrakech, Morocco,

²Geoenvironment, Georesources and Civil Engineering Laboratory, FST, UCA, Marrakech, Morocco

* Corresponding author: aicha.fadil1974@gmail.com

Article History:

Received: August 4, 2025

Revised: September 25, 2025

Accepted: October 6, 2025

Published: October 30, 2025

Abstract: Morocco's climate is predominantly semi-arid and arid, with 93% of its territory falling under these classifications. Land degradation poses a significant environmental risk, particularly in the mountainous regions of the High Atlas. These areas are marginalized in development and economic growth, with an average soil loss of 35 t. ha⁻¹. yr⁻¹ according to REEM, 2015. The severity of this phenomenon is expected to escalate due to the interplay of natural and anthropogenic factors, often exacerbated by unsustainable resource management and exploitation practices. Among the various forms of water-induced soil erosion, gully erosion is the most dynamic and destructive, adversely affecting the land and the livelihoods of local populations in mountainous regions, such as the Rhéraya watershed in the Western High Atlas. Mitigating this degradation process and addressing its impacts are critical for reducing local vulnerabilities and enhancing the resilience of socio-ecological systems. Effective risk reduction necessitates the adoption of decision-making tools tailored to specific territories, enabling comprehensive diagnostics and prioritization of intervention areas based on severity. This study aims to systematically classify gully erosion risk within the Rhéraya watershed using an ordinal scale. The risk assessment integrates two components: hazard and vulnerability, evaluated through indicators aggregated via multi-criteria analysis (MCA). These indicators encompass biophysical factors (e.g., land use, slope inclination and length, rock friability, and soil type) and social dimensions (e.g., human, infrastructural, and economic stakes associated with soil degradation). The methodology draws



Copyright: © 2025 by the authors. Licensee JHU

This article is an open-access article distributed under the terms and conditions of the Creative Commons Attribution License (<http://creativecommons.org/licenses/by/4.0>)

inspiration from the SCALES model (Spatialisation d'échelle fine de l'ALéa d'Erosion des Sols), the Analytic Hierarchy Process (AHP), and spatial modelling techniques using Geographic Information Systems (GIS). The developed model serves as a strategic tool for soil conservation and restoration efforts, protecting environmental goods and services while bolstering the resilience of local communities. Key outcomes include a systematic territorial classification highlighting gully erosion risk and its implications for both environmental and socio-economic assets. The main objective of this study is to assess the vulnerability to soil erosion in the Riraya basin by implementing a multi-criteria methodology for evaluating erosion risks, taking into account the characteristics of erosion risk and vulnerability in order to create a comprehensive system for diagnosing and monitoring the state of erosion in the watershed, which makes it possible to identify the areas at risk that need to be protected as a priority. In light of the results obtained, the risk of gully erosion appears to be active and significant across more than half of the watershed (51.20% of the area, or 11,531 ha), with fairly high hazard and vulnerability rates. The accuracy rate was estimated at approximately 86.67%, which guarantees the reliability of the results obtained and the validity of this model in estimating erosion risk.

Keywords: gully erosion, risk, AHP multi-criteria analysis, Riraya watershed, SCALES model.

基于多准则分析的沟蚀风险评估：以乌德·雷拉亚流域为例

摘要：摩洛哥气候以半干旱和干旱为主，93%的国土属于此类气候类型。土地退化构成重大环境风险，尤其在高阿特拉斯山脉山区。这些地区在发展和经济增长中处于边缘化地位，据REEM（2015）数据显示，平均土壤流失量达35吨/公顷·年。受自然与人为因素共同作用，加之资源管理与开发实践不可持续，该现象的严重程度预计将持续加剧。在各类水蚀侵蚀形态中，沟蚀最具动态破坏性，对西部高阿特拉斯山脉雷拉亚流域等山区土地及当地居民生计造成严重影响。缓解此类退化进程并应对其影响，对降低区域脆弱性、增强社会生态系统韧性至关重要。有效的风险降低需要采用针对特定区域定制的决策工具，以实现基于严重程度的综合诊断和干预区域优先排序。本研究旨在运用序数尺度对雷拉亚流域沟蚀风险进行系统分类。该风险评估整合了危害与脆弱性两个维度，通过多准则分析（MCA）聚合指标进行综合评价。这些指标涵盖生物物理因素（例如土地利用、坡度倾斜度和坡长、岩石脆性、土壤类型）和社会维度（例如与土壤退化相关的人类、基础设施和经济利益）。该方法借鉴了SCALES模型（土壤侵蚀风险精细化空间化模型）、层次分析法（AHP）以及基于地理信息系统（GIS）的空间建模技术。该模型作为土壤保护与修复工作的战略工具，既守护环境公共产品与服务，又增强社区韧性。核心成果包括建立系统性区域分类体系，重点标识沟蚀风险及其对环境与社会经济资产的双重影响。本研究的主要目标是通过实施多准则评估法，结合侵蚀风险与脆弱性的特征，评估里拉亚流域的土壤侵蚀脆弱性，从而建立一套全面的流域侵蚀状态诊断与监测体系，进而识别出需要优先保护的风险区域。根据分析结果，超过半数流域区域（占总面积51.20%，即11,531公顷）存在活跃且显著的沟蚀风险，其灾害发生率与脆弱性指标均处于较高水平。模型准确率约为86.67%，确保了研究结果的可靠性及该模型在侵蚀风险评估中的有效性。

关键词：沟蚀、风险、AHP多准则分析、雷拉亚流域、SCALES模型。

1. Introduction

Gully erosion represents an advanced stage of linear erosion, characterized by the formation of deep channels caused by the accumulation of runoff water, which removes topsoil to a significant depth [1]. This process poses severe risks to both natural and socio-economic systems [2]. In the Mediterranean region, including Morocco, the risk of gully erosion has intensified due to the interplay of biophysical characteristics, such as climate irregularities, lithology, and soil properties, as well as anthropogenic

activities associated with land use and management practices.

Gully erosion is a dominant contributor to sediment yield in arid and semi-arid regions, accounting for an average of 60% of the solid load mobilized by water erosion [3]. Morocco's mountainous regions have experienced significant soil degradation over the 20th century due to water erosion, with soil loss rates averaging 20 t·ha⁻¹·yr⁻¹ in the Rif and 5-10 t·ha⁻¹·yr⁻¹ in the Middle and High Atlas [4, 5]. These erosive

processes have had substantial impacts on both physical environments and human activities [6].

In the High Atlas Mountains, which encompass the Rhéraya watershed, gully erosion exacerbates the silting of dams, diminishes soil productivity, and damages infrastructure [7, 8]. This watershed is characterized by steep slopes, a complex and fragile lithological structure, and a highly variable rainfall regime. It is particularly vulnerable to water erosion, with gully erosion intensified by heavy thunderstorms and torrential floods that frequently occur in summer and early autumn. These extreme events result in considerable damage, including loss of life, habitat destruction, and infrastructure degradation [9]. Mitigating the impacts of gully erosion requires the use of decision-support tools for comprehensive diagnostics and the identification of priority intervention areas. Spatial analysis and mapping techniques enable the visualization of the location, extent, and probability of erosive phenomena. Moreover, employing a consistent and homogeneous methodology across the study area allows for the identification and ordinal ranking of at-risk areas according to their severity.

This study aims to systematically rank the gully erosion risk within the Rhéraya watershed using an ordinal scale. Risk assessment is conducted through the aggregation of biophysical (e.g., land use, slope inclination and length, rock friability, soil type) and social (e.g., human and infrastructural concerns) indicators using a multi-criteria evaluation (MCE) approach. The methodology is inspired by the semi-quantitative SCALES model (Spatialization at a Fine Scale of Soil Erosion Risk).

The results provide a classification of the territory, particularly highlighting the gullies and their associated risks to the environment and the local population. The generated risk map, derived from applying the SCALES model, was subsequently validated through field observations to ensure the reliability of the findings.

2. Methods and materials

2.1. Study area

The Rhéraya watershed is situated between the axial zone of the Western High Atlas in the south and the Oued Tensift in the north (*Figure 1*).

Geographically, it lies within the rectangular coordinates defined by the intersection of meridians 8° and 7.48° west and parallels 31.18° and 31.02° north. The watershed spans an area of 223.92km^2 with a perimeter of 78km . Its hydrographic network is well branched, extending 32 km and yielding a drainage density of approximately $3.8\text{km}\cdot\text{km}^{-2}$. The main river's average gradient is 7.2% . The watershed's physiognomy is characterized by bifurcation (Imlil and Iménane) and rugged topography, resulting in a

time of concentration (T_c) of around 4 hours and 30 minutes, as calculated using the Giandotti formula. Additionally, its relatively elongated shape is quantified by the Gravelius compactness index $K_g=1.46K_g$, which facilitates the concentration and acceleration of flow velocities along the slopes.

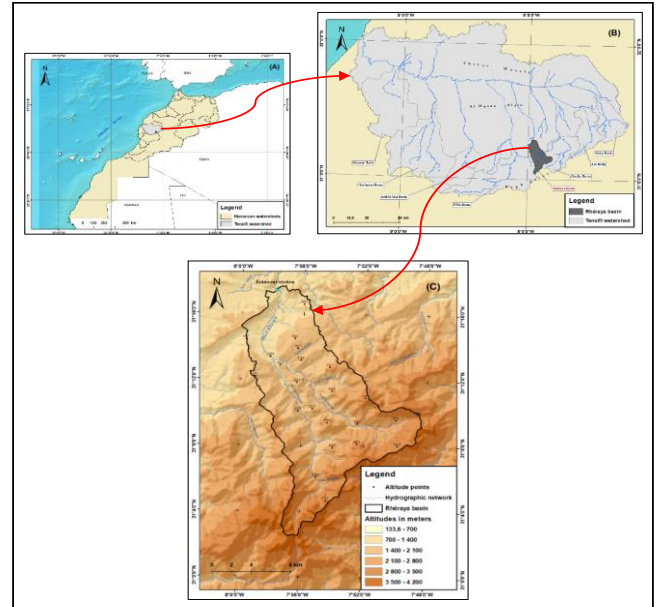


Figure 1. Geographical location of the Rhéraya watershed: National scale (A), Regional scale (B), and Local scale (C)

Hydrologically, the Rhéraya river system consists of two primary rivers: Oued Iménane in the east and Oued Imlil in the west. These rivers converge downstream to form Oued Rhéraya (*Figure 2*) after traversing two-thirds of the watershed.

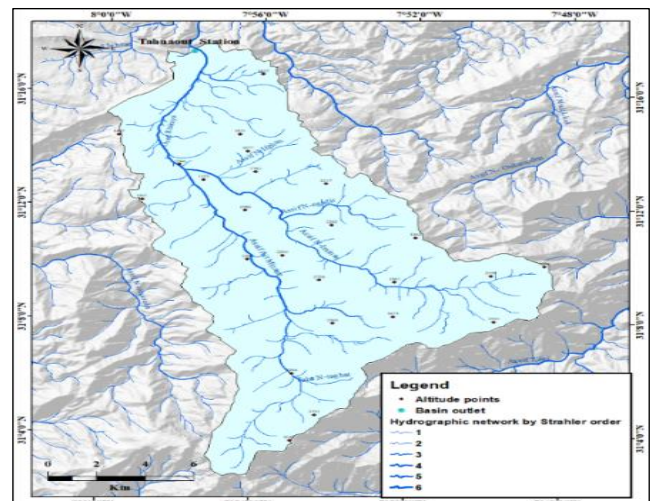


Figure 2. Hydrographic network map illustrating the primary rivers and drainage patterns of the Rhéraya watershed

Upstream, the Rhéraya river system is more extensively branched due to the diverse geological features at medium and high altitudes, especially on the right bank of Oued Iménane and the left bank of Oued Imlil. In the downstream segment, at the confluence of the Iménane and Imlil rivers, flood

events become more severe. This increased flood risk arises from the gentler terrain relief and the accumulation of surface water from the entire watershed [10]. Climatically, the study area experiences a semi-arid environment marked by an aggressive rainfall pattern.

This includes heavy, concentrated showers during the summer and prolonged, low-intensity rain in the winter. The annual average rainfall is approximately 378mm, as recorded at the Tahanaout station (elevation: 1064m) for the period 1971-2017.

Rainfall data for this period highlight substantial variability between hydrological years, with differences exceeding 450mm between the wettest and driest years. The intensity of erosion in the region is influenced not only by total annual precipitation but also by its temporal distribution.

The Rhéraya watershed experiences two distinct seasons: a dry season from June to September, with July being the driest month, and a rainy season from October to May, with April being the wettest month (average rainfall: 55.67mm). This pronounced spatio-temporal variability in rainfall, both annual and monthly, is a critical climatic factor driving erosion. Moreover, the basin exhibits notable spatial rainfall variation, often correlated with altitude, further amplifying the complexity of erosive processes within the watershed.

The vegetation cover of the Rhéraya watershed can be categorized into three predominant land-use types that define the region's landscape: natural vegetation, which includes cedar forests at lower altitudes and mixed juniper and holm oak at higher elevations; irrigated croplands concentrated along the two main branches of the Rhéraya River; and bare land, prevalent at the highest altitudes.

A land cover map (Figure 3A) was generated through supervised classification of a Sentinel 2 satellite image acquired in June 2020. This image, recorded across 13 spectral bands with a spatial resolution of 10 meters, provided a detailed representation of the landscape. The accuracy of the resulting map was validated using field reconnaissance data collected from 80 control points, achieving an overall accuracy rate of approximately 89.42% (Table 1).

Table 1. Accuracy assessment of land use classification in the Rhéraya watershed based on field validation data (Developed by the authors)

Class	Crops	Forests	Buildings	Matorrals	Sparse Vegetation	Bare Ground/ Rock Outcrop
Accuracy Rate (%)	83	80	100	82	91	100

The topography of the Rhéraya watershed is notably rugged, with elevations ranging from 1103 to 4207 m above sea level. Slope gradients vary significantly, from 0° on the downstream terraces to as steep as 62° on upstream slopes (Figure 3B). Slope lengths, calculated using the formula by Moore and Burch (1986), range from 0 to 79 m (Figure 3C). This variability in slope distribution directly influences the hydrological regime and overall erosive dynamics of the watershed.

From a geological perspective, the Rhéraya basin is underpinned by a Hercynian basement overlaid by formations from the Mesozoic and Cenozoic eras. The geological formations can be grouped into three main categories (Figure 3D):

- Impermeable formations, such as granites and magmatic rocks, cover 59% of the area.
- Limestone formations constitute 26% of the basin.
- Sandstone-clay formations, which make up the remaining 15% [11].

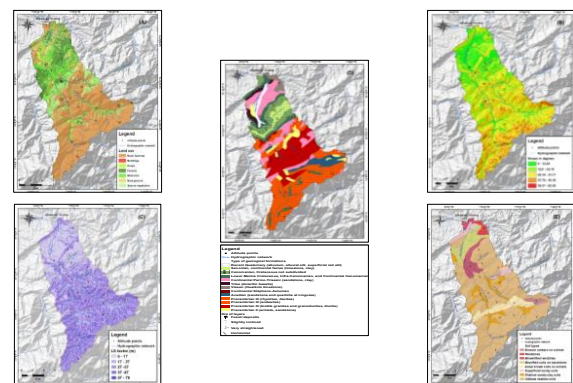


Figure 3. Spatial distribution of biophysical factors in the Rhéraya basin: (A) Land use, (B) Slope degree, (C) Slope length, (D) Rock friability, and (E) Soil type

The predominance of impermeable formations contributes to rapid and intense flood events, exacerbating erosion processes [9].

Soil characteristics within the Rhéraya watershed are diverse yet largely undeveloped, apart from certain forested areas and developed terraces. The Haouz plain, adjacent to Oued Rhéraya, features fersiallitic soils typical of Mediterranean environments [12]. These reddish, clayey soils are highly susceptible to wind and water erosion [13] due to their iron content. Upstream of Tahanaout, these soils transition to piedmont soils overlying Tertiary formations. Between Tahanaout and Asni, rendosols young, shallow soils rich in organic matter, are prevalent, often in association with limestone layers. High-altitude zones are dominated by skeletal soils with minimal development due to low temperatures, as well as sandy and brown clay soils [11].

Given the lack of detailed soil maps for the region, the geological map was adapted to produce a

simplified pedological classification. This classification draws from the pedological maps developed by CHAPONNIÈRE, A. 2005 and OUCHALA, M. 2021, defining eight soil classes based on textural characteristics (Figure 3E).

The Rhéraya watershed has undergone significant socio-economic changes, particularly between 2000 and 2010, driven by tourism and urban development. The distribution of the population (Figure 4A) across the basin has contributed to the encroachment of urban areas onto natural and agricultural lands, intensifying conflicts between land use and environmental conservation.

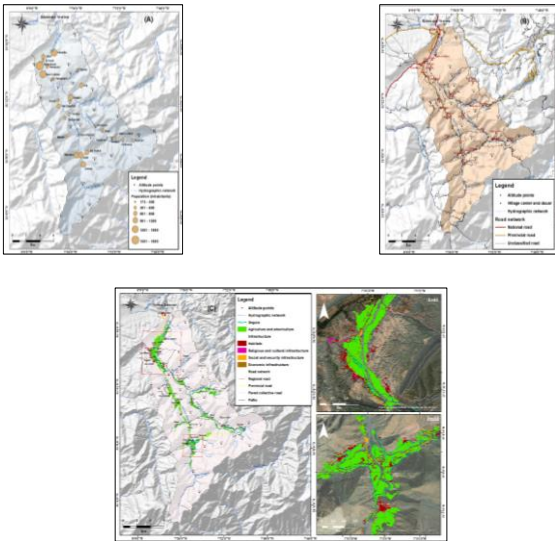


Figure 4. Spatial distribution of populations (A) and infrastructures (B, C) in the Rhéraya basin

The watershed hosts diverse infrastructure types (Figures 4B and 4C), including: Social and security infrastructure, such as schools and law enforcement facilities; economic infrastructure, including markets and transportation links; religious and cultural establishments, as well as water, sanitation, and agricultural facilities (e.g., orchards and water sources).

These infrastructural developments and their interactions with the natural environment exacerbate soil erosion risks, highlighting the need for integrated management strategies.

2.2. Data and research methods

The adopted modeling approach is inspired by the SCALES model developed by the Geophen laboratory at the University of Caen, France [14]. This model employs a method of cross-referencing parameters influencing gully erosion through logical combinations to estimate erosion risks spatially. The model incorporates nine key parameters, categorized as follows: biophysical parameters (Land use, Rock friability, Soil type, Slope length, Slope degree) and socio-economic parameters (Population density, Arboriculture, Road network, Social facilities).

The climatic factor, specifically precipitation, was excluded from the model. In semi-arid climates with episodic heavy rainfall, the probability of erosive events is uniformly distributed across the watershed. Consequently, precipitation is considered constant for this analysis.

The selected parameters were prioritized and weighted using current knowledge of erosion processes. The semi-quantitative model is structured as a logical tree diagram (Figure 5) and implemented in a GIS environment. Each parameter was represented as an information layer in the GIS and qualitatively reclassified based on its sensitivity to erosion. This reclassification process involved assigning weights to the sensitivity of parameter classes, guided by prior research [15, 16].

To combine the layers and determine their overall contribution to erosion risk, a hierarchical multi-criteria analysis (AHP) was employed [17]. The AHP methodology involves pairwise comparisons of parameters to assess their relative importance. This is done by constructing a square matrix where each parameter is compared to others using a predefined scale. Two levels of weight assignments are required:

*Class Level: Determining the erosion sensitivity index of each parameter's classes.

*Criteria Level: Assigning weighting coefficients to each criterion based on its influence on gully risk.

Weights for parameter sensitivity and class sensitivity were derived based on expert opinions from specialists in erosion processes. These expert judgments were validated through comparisons with existing literature and alignment with the environmental conditions of the study area.

The accuracy of the data was ensured through rigorous construction of comparison matrices at both the class and criteria levels. This approach facilitated the reliable estimation of gully risk.

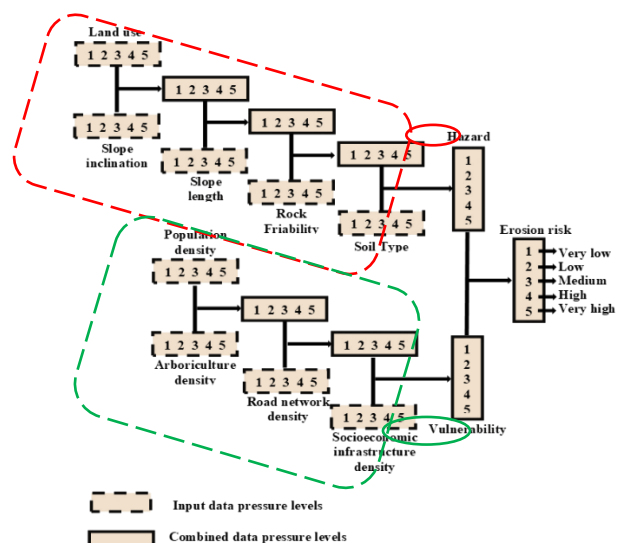


Figure 5. Diagram illustrating the logical tree structure of the SCALES model (Developed by the authors)

2.2.1. Data

The methodological approach employed in this study is based on a comprehensive dataset, designed to describe the environmental characteristics, assess the stakes involved, and identify the relevant variables for risk estimation. Several data pre-processing steps were required to standardize and harmonize the dataset, ensuring its suitability for the development of the risk model. The data sources utilized in this research include:

*Digital Terrain Model (DTM): A DTM with a resolution of approximately 12.5m was used to extract detailed information on terrain morphology, such as slope degree and length.

*Sentinel-2 Satellite Imagery (June 2020): Sentinel 2 imagery was employed to delineate the study area and classify different types of land use.

*1/500000 Geological Map of Morocco: This map was utilized to assess the distribution of lithological units within the watershed and to evaluate the permeability and erodibility of the surface.

*Topographic Maps (1/50000) of Tahnaout and Toubkal, and Google Earth High-Resolution Imagery: These resources were used to extract information on the location of main settlements and village infrastructures, enabling an analysis of socio-economic factors.

*Soil Data: Soil data were incorporated to determine the type and characteristics of the soils within the study area.

*Statistical Data on Social Aspects (Communal Level): Statistical data, sourced from the General Population and Housing Census in 2014, were used to analyze demographic and socio-economic variables relevant to the study.

2.2.2. Determining erosion risk

In general, risk is defined as the product of hazard and vulnerability [2]. To determine the gully erosion risk, thematic maps of the selected factors were cross-referenced in pairs, as illustrated in Figure 5. This process generated two distinct maps: the first, referred to as the *hazard map*, and the second representing *vulnerability* along with the associated stakes. Each

combination of factors was assigned a sensitivity weight regarding gully erosion. The hazard map was then multiplied [18] by the vulnerability map to produce the final gully erosion risk map:

$$\text{Risk} = \text{Hazard} \times \text{Vulnerability} \quad (1)$$

2.2.3. Determining the erosive hazard

The assessment of erosive hazard is based on five criteria, the combination of which allows for an evaluation of the overall hazard. The model's hierarchical tree structure prioritizes factors that are subject to human disturbance. These factors, listed in descending order of importance, are land use, slope steepness, slope length, rock friability, and soil type (Figure 6).

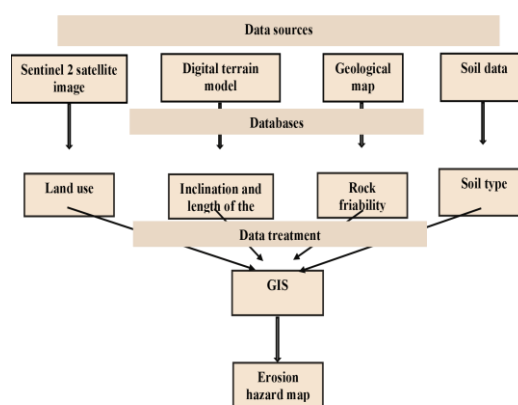


Figure 6. Organizational chart of the erosion risk indicator (Developed by the authors)

The classification of erosive hazard levels is derived from the aggregation of erosion sensitivity indices assigned to the classes of these criteria (Table 2). These indices were determined based on expert judgment, specifically from faculty members of the Geoenvironment, Georesources, and Civil Engineering Laboratory at Cadi Ayyad University, Marrakech. The expert opinions were corroborated with data from the literature [19, 20, 21]. For effective data management, all thematic maps were resampled to match the 12.5m resolution of the satellite imagery utilized in this study.

Table 2. Weights assigned to each class for different erosive criteria (Developed by the authors)

Land Use	Bare Soil/ Rocky Outcrops	Crops	Built-Up Areas	Sparse Vegetation	Forests/ Matorrals	Total	Erosion Sensitivity Index
Bare Soil/Rocky Outcrops	1	3	5	7	9	25	0.52
Crops	0.33	1	3	2	3	9.33	0.20
Built-Up Areas	0.2	0.33	1	3	2	6.53	0.14
Sparse Vegetation	0.14	0.2	0.33	1	3	4.67	0.10
Forests/Matorrals	0.11	0.33	0.2	0.33	1	1.97	0.04
						47.5	1

Slope inclination (%)	50–63	38–50	25–38	13–25	0–13	Total	Erosion Sensitivity Index
50–63	1	3	5	6	9	24	0.47
38–50	0.33	1	3	4	5	13.33	0.26
25–38	0.20	0.33	1	1.5	5	8.03	0.16
13–25	0.17	0.25	0.67	1	1.5	3.59	0.07
0–13	0.11	0.20	0.20	0.67	1	2.18	0.04
						51,13	1

Slope Length (m)	47–79	37–47	27–37	17–27	0–17	Total	Erosion Sensitivity Index
47–79	1	1.5	3.5	7	9	22	0.45
37–47	0.67	1	1.5	3	5	13.5	0.27
27–37	0.33	0.67	1	1.5	3	7.75	0.16
17–27	0.20	0.33	0.67	1	1.5	3.91	0.08
0–17	0.14	0.20	0.33	0.67	1	2.02	0.04
						49,18	1

Soil Type	Ferralsols	Sandy Soils	Rankers	Rendosols	Skeletal Soils	Total	Erosion Sensitivity Index
Ferralsols	1	2	4	5	7.5	19.5	0.38
Sandy Soils	0.5	1	3	5	6	15.5	0.30
Rankers	0.25	0.33	1	3	5	9.58	0.19
Rendosols	0.2	0.20	0.33	1	3	4.73	0.09
Skeletal Soils	0.13	0.17	0.20	0.33	1	1.83	0.04
						51,14	1

Rock Type	Clay/Sandstone/Quaternary	Marl-Limestone	Basalt/Schist	Limestone	Granite/Rhyolite	Total	Erosion Sensitivity Index
Clay/Sandstone/Quaternary	1	3	4	4	6	18	0.46
Marl-Limestone	0.33	1	1.5	2	4	8.83	0.23
Basalt/Schist	0.25	0.67	1	1.5	2	5.42	0.14
Limestone	0.25	0.5	0.67	1	1.5	3.92	0.10
Granite/Rhyolite	0.17	0.25	0.5	0.67	1	2.59	0.07
						38,76	1

These maps were then integrated into a Geographic Information System (GIS) environment, with the final hazard equation expressed as:

Hazard = $\alpha P_1 + \beta P_2 + \gamma P_3 + \delta P_4 + \varepsilon P_5$ (2)
 With: P_1, P_2, P_3, P_4, P_5 represent the five criteria (land use, slope inclination, slope length, rock friability, and soil type), and $\alpha, \beta, \gamma, \delta, \varepsilon$ are their respective weights (Table 3).

Table 3. Weighting of different erosive hazard criteria (Developed by the authors)

Criteria	Land Use	Slope Inclination	Slope Length	Rock Friability	Soil Type	Total Weight	Weighting Coefficient
Land Use	1	1.39	1.67	2.38	2.60	9.04	0.31
Slope Inclination	0.73	1	1.54	2.13	2.27	7.67	0.26
Slope Length	0.63	0.65	1	1.5	1.82	5.60	0.19
Rock Friability	0.43	0.48	0.67	1	1.59	4.17	0.14
Soil Type	0.37	0.45	0.55	0.58	1	2.95	0.10
						29,43	1

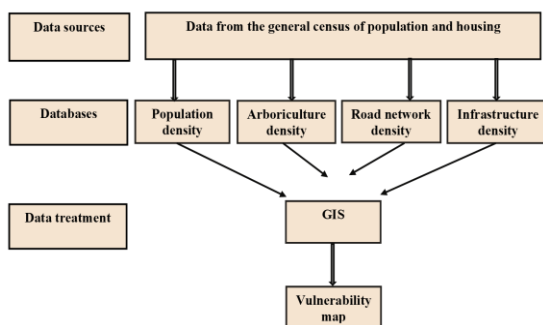
2.2.4. Determining vulnerability

For a long time, risk management focused primarily on understanding and controlling the hazard. However, the concept of vulnerability, which is now recognized by various scientific disciplines as well as local stakeholders and elected representatives, has recently emerged as an independent field of study [22]. Vulnerability is associated with the elements exposed to a hazard and encompasses human lives, activities, infrastructures, and socio-economic facilities (Figure 7).

Vulnerability classes are derived from the sum of erosion sensitivity indices assigned to the different parameter classes based on both literature data and environmental knowledge (Table 4). Each index is multiplied by the weighting coefficient of the corresponding thematic layer (parameters):

$$\text{Vulnerability} = \lambda V_1 + \sigma V_2 + \mu V_3 + \phi V_4 \quad (3)$$

Where: V_1 to V_4 are the parameter maps, and $\lambda, \sigma, \mu, \phi$ are their respective weighting indices, corresponding to population density, tree density, road network density, and socio-economic infrastructure density (Table 5).



Figure

7. Organizational chart of the vulnerability indicator

Table 4. Weights assigned to each class of vulnerability criteria (Developed by the authors)

Population Density (inhabitant/km ²)	366-552	251-366	154-251	65-154	0-65	Total	Index Sensitivity to Erosion
366-552	1	3	5	7	9	25	0.51
251-366	0.33	1	3	4	6	14.33	0.27
154-251	0.2	0.33	1	2	3	6.53	0.13
65-154	0.14	0.25	0.33	1	1.5	3.22	0.06
0-65	0.11	0.17	0.25	0.33	1	1.86	0.03
						50,94	1

Arboriculture Density (Number/km ²)	90-142	56-90	30-56	10-30	0-10	Total	Index Sensitivity to Erosion
90-142	1	1.5	2	2.5	3	10	0.34
56-90	0.67	1	1.5	2	2.5	7.67	0.25
30-56	0.5	0.67	1	1.5	2	5.67	0.18
10-30	0.4	0.5	0.67	1	1.5	4.07	0.13
0-10	0.33	0.4	0.5	0.67	1	2.90	0.10
						30,31	1

Road Network Density (km/km ²)	24-33	18-24	13-18	7-13	0-7	Total	Index Sensitivity to Erosion
24-33	1	2	4	5	7	19	0.42
18-24	0.5	1	2	4	5	12.5	0.27
13-18	0.25	0.5	1	2	4	7.75	0.17
7-13	0.2	0.25	0.5	1	2	3.95	0.09
0-7	0.14	0.2	0.25	0.5	1	2.09	0.05
						45,29	1

Socioeconomic Infrastructure Density (Number/km ²)	44-77	26-44	12-26	4-12	0-4	Total	Index Sensitivity to Erosion
44-77	1	2	3	4	5	15	0.51
26-44	0.5	1	2	3	4	10.5	0.22
12-26	0.33	0.5	1	2	3	6.83	0.14
4-12	0.25	0.33	0.5	1	2	4.08	0.08
0-4	0.2	0.25	0.33	0.5	1	2.28	0.05
						48,69	1

Table 5. Weighting of different vulnerability criteria (Developed by the authors)

Criteria	Population density	Arboriculture density	Road network density	Socioeconomic infrastructure density	Total weight	Weighting index
Population density	1	1.5	2	3	9	0.39
Arboriculture density	0.67	1	1.5	2.5	5.33	0.29
Road network density	0.5	0.67	1	1.5	3.67	0.19
Socioeconomic infrastructure density	0.33	0.4	0.67	1	1.45	0.13
					15,78	1

3. Results

3.1. Mapping erosion hazard factors

The analysis of physical factors contributing to erosion was conducted by subdividing all maps into five sensitivity classes for gully erosion. The land use map produced shows that the dominant class is bare soil and rock outcrops, occupying half of the watershed, or around 61.78% (13900 ha) of the total area. Whereas the sparse vegetation, dense vegetation, and cultivated land classes are mainly distributed in the downstream catchment and adjacent to the wadi and its main watercourses, occupying 38.22% (8600 ha) of the area, reflecting low land cover and an increase in the area vulnerable to gully erosion within the catchment. According to the generated slope map, the steepest to moderate slopes (25-63°) cover 59.86% (13500 ha) of the total watershed area, while low to very low slopes (0-25°) dominate only 39.5% (9000ha). For the slope length map produced, almost the entire area is

dominated by the steepest to moderate classes (27-79°), which account for around 90.93% (20460 ha) of the watershed, while the low to very low classes (0-27°) cover just 9.07% (2040ha). Judging by the material friability map obtained, the most erodible soils (vulnerable, very vulnerable, and moderately resistant materials) are largely located in the center and downstream of the watershed, occupying around 47.82% (10760 ha) of the total area.

While weak to extremely weak lithofacies represent only 52.18% (11740 ha). Based on the soil type map generated, very high to moderate gully-susceptible soils cover 26.29% (6020 ha), while low to very low classes dominate the watershed, accounting for around 73.71% (16480 ha) of the total watershed area (cf. *Figure 8*).

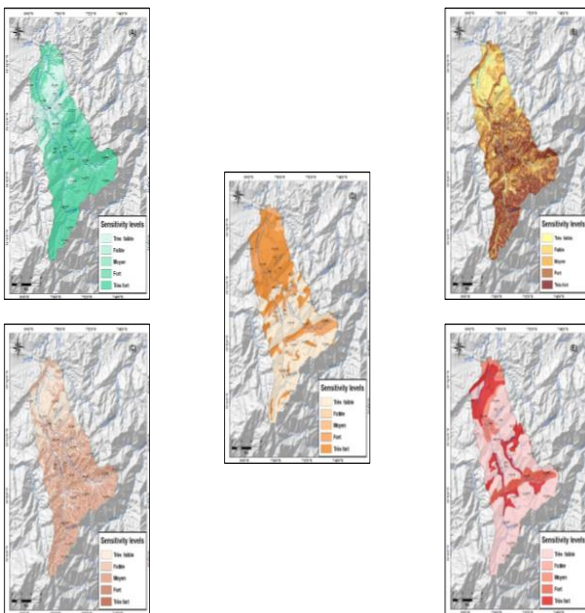


Figure 8. Spatial distribution of erosive hazard classes based on sensitivity factors: land use (A), slope gradient (B), slope length (C), rock friability (D), and soil type (E)

The weighted superimposition of the five maps of parameters acting on land degradation according to the chosen model yielded the erosive hazard map, providing information on erosive hazard classes in the Rhéraya catchment area graded into five levels: very low, low, medium, high and very high with different surface areas (*Figure 10A*). Overall, areas with medium to very high erosion hazard occupy 64.23% (14450 ha) of the total area of the Rhéraya watershed. These more erodible regions correspond in particular to land in the north-western part with a fairly high soil friability rate, dominated by clays and marl limestones, a low to very low vegetation cover rate marked by the presence of crops and bare soil, and soils more sensitive to gully erosion, particularly fersiallitic soils. These areas also coincide with almost two-thirds of the upstream part of the basin, which is characterized by very steep slopes in degree and length, and almost zero vegetation cover.

3.2. Mapping vulnerability factors

The integration of four vulnerability maps addressing human life issues, arboriculture and hydro-agricultural equipment, road network issues, and other infrastructural concerns (*Figure 9*) was conducted within a GIS environment in accordance with the SCALES model framework. This process produced the comprehensive vulnerability map (*Figure 10B*). The resulting map reveals that areas classified as extremely to moderately vulnerable constitute 26.23% (590 ha) of the watershed. These areas are characterized by elevated index values across nearly all social factors, including population density, arboriculture, hydro-agricultural equipment, road networks, and other socio-economic

infrastructures. Geographically, these vulnerable zones are concentrated downstream, particularly in the vicinity of the Asni center and along the hydrographic network traversing the watershed. Prominent hotspots include and surround the centers of Imi Oughlad, Imlil, and Ouanesekra.

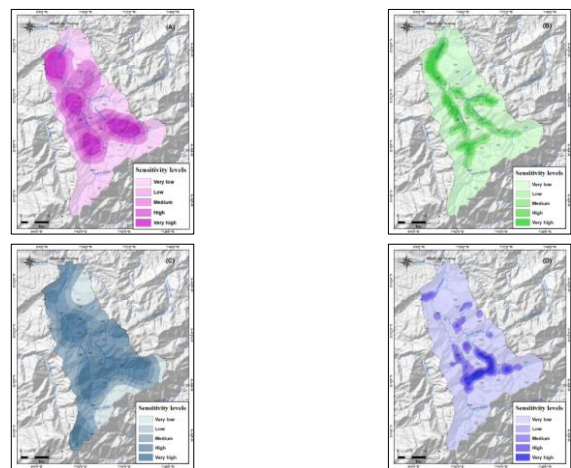


Figure 9. Spatial distribution of vulnerability criteria based on sensitivity factors: population density (A), arboriculture density (B), road network density (C), and infrastructure density (D) (Developed by the authors)

These vulnerable regions are preferentially occupied by farming communities and are the primary recipients of hydro-agricultural and socio-economic investments. Conversely, areas with low to very low vulnerability are evident across 73.77% (16598 ha) of the Watershed. Sparse or nonexistent populations and minimal infrastructure development mark these regions.

3.3. Mapping the risk of gully erosion

The gully erosion risk map was developed by integrating the erosive hazard map with the vulnerability map (*Figure 10C*). This analysis delineated five gully erosion risk classes: very low, low, medium, high, and very high. The resulting map highlights that areas with high gully erosion risk are predominantly associated with regions exhibiting elevated levels of both erosive hazard and vulnerability.

Active gully erosion, encompassing medium, high, and very high-risk levels, is evident across more than half of the catchment area, covering 51.20% of the surface (11531ha). Areas experiencing moderate to severe gully erosion are concentrated around the centers of Asni, Imlil, and Ouanesekra. These zones are particularly susceptible due to a combination of factors, including predominance of soils with low to very low vegetation cover, very steep slopes, highly friable rocks and soils, notably fersiallitic and sandy types, with significant susceptibility to erosion, high densities of socio-economic elements such as population, arboriculture, and hydro-agricultural infrastructure.

These factors collectively amplify the vulnerability of these regions to gullying, underscoring the need for targeted mitigation strategies.

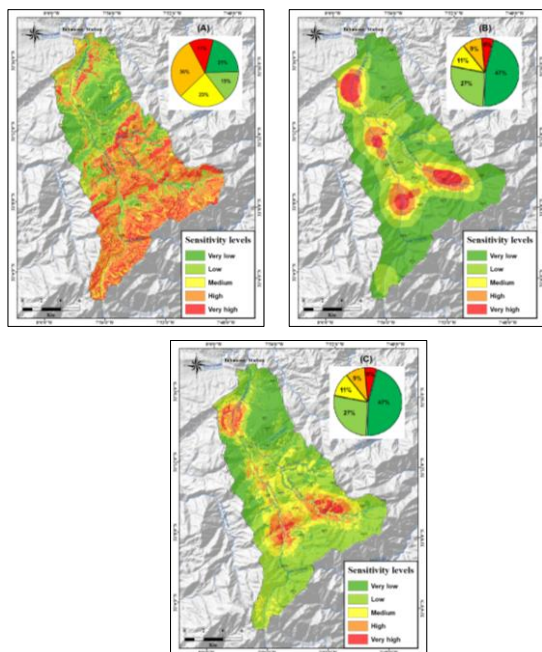


Figure 10. Spatial distribution of erosive hazard (A), vulnerability (B), and gully erosion risk (C) levels within the Rhéraya watershed (Developed by the authors)

4. Discussions

The interpretation of the erosion risk map reveals a dispersed spatial distribution of gully erosion classes, indicating that all contributing factors act synergistically to exacerbate soil degradation. A comparative analysis of biophysical and socio-economic parameter maps across the study area is essential for a comprehensive understanding of gully erosion mechanisms and accurate interpretation of the risk classification.

Field visits, surveys with local populations, and a review of the existing literature on gully erosion modeling, particularly in arid and semi-arid regions, underscore the significant influence of physio-natural factors on gully erosion. The key factors, ranked by their importance, include vegetation cover, slope gradient, rock friability, and soil type, aligning with the prioritization used in the semi-quantitative model. Among socio-economic factors, population density, road network density, and arboriculture were identified as the most impactful drivers of erosive phenomena.

Comparing the erosion risk map with the land use map highlights critical patterns. In the northern and northeastern regions of the basin, areas dominated by dense forest exhibit very low erosion risk. Similarly, zones covered with matorral and sparse vegetation demonstrate low susceptibility to gully erosion due to the protective effect of vegetation against soil degradation. In contrast, cultivated and bare lands in the

northwestern and southern parts of the basin are associated with high to very high erosion risk classes.

Further analysis reveals that medium to very high erosion risk areas are predominantly found in regions with steep to very steep slopes. This association suggests that slope steepness and the kinetic energy of runoff over long slopes are critical factors driving erosion. The influence of topography is especially evident in areas where steep slopes coincide with bare or severely degraded vegetation, as observed around Imlil and Ouansekra. A positive relationship between slope gradient and erosion rates is evident on degraded and bare lands, with topography significantly amplifying gullying processes in these areas.

However, the highest gullying risk classes are not solely attributable to slope. An examination of the geological map identifies the presence of friable formations, such as clays, marls, and limestones, which contribute to erosion by varying water infiltration capacities, modulated by vegetation cover, porosity, and surface sealing [23]. Soil type also plays a crucial role, with erosion susceptibility determined by soil permeability, detachment potential, and particle transport. In the study area, soils such as fersiallitic, sandy, and Rankers, in combination with steep slopes, are highly prone to gullying due to their susceptibility to rainfall impact and runoff shear forces, influenced by their texture, structure, porosity, and organic matter content.

Conversely, areas in the foothills and high mountains exhibit low gullying susceptibility despite steep slopes and sparse vegetation. This resilience is attributed to the compact and resistant nature of the substrate materials. Low gully erosion risk in these regions is also associated with minimal socio-economic activity, as indicated by the absence of socio-economic vulnerability factors.

The correlation between vulnerability and gully erosion risk is evident, with high-risk areas corresponding to regions of moderate to very high vulnerability. This aligns with the assertion that "without men, there is no disaster" [24]. Thematic maps confirm that high socio-economic vulnerability, characterized by dense populations, road networks, arboriculture, and hydro-agricultural facilities, is a critical determinant of elevated erosion risk.

Despite its strengths, the multi-criteria approach to erosion assessment has limitations that may constrain its application. A major challenge lies in the subjective selection of parameters and their assigned weights, which introduces variability and difficulty in accounting for the temporal dynamics of erosive processes. Additionally, key data necessary for evaluating vulnerability components, such as specific land use patterns and official soil maps, are often unavailable from public or governmental sources.

To address these limitations and enhance the reliability of the semi-quantitative SCALE based erosion risk assessment, it is imperative to validate the resulting erosion risk map through empirical or quantitative methods.

5.Validation of the semi-quantitative model

The validation of the erosion risk map, developed using the semi-quantitative SCALE model, is essential to ensure the reliability of the results. This process involved in situ verification at 15 control points distributed across the basin (Figure 11), representing all erosion risk classes, with three control points assigned to each class.

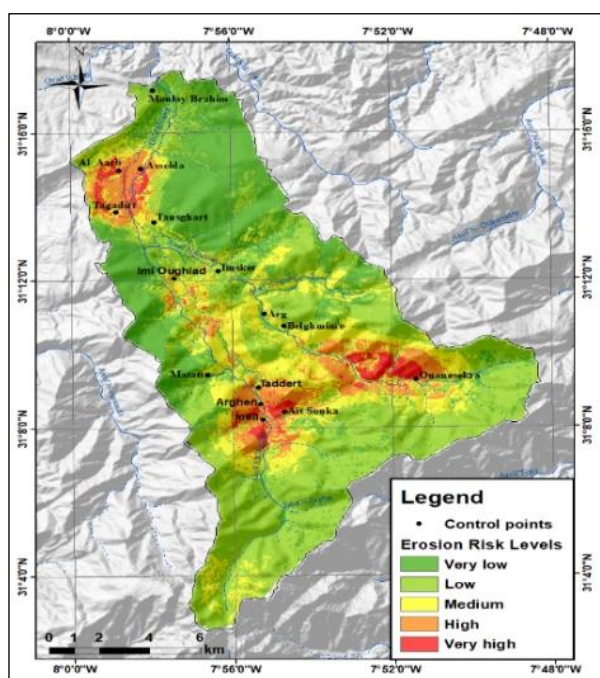


Figure 11. Control points used to validate the semi-quantitative SCALE model

Of the 15 control points, two were found to be inconsistent with field observations (Table 6). These points, located in Moulay Brahim and Al Aarb, were classified as having high and very high erosion risk levels, respectively. Field investigations, corroborated by accounts from local residents, revealed that these discrepancies were primarily driven by anthropogenic activities.

In Al Aarb, the presence of non-native residents engaging predominantly in livestock farming has exerted significant pressure on the surrounding forests. Similarly, in both villages, deforestation and overgrazing have severely degraded the soils. Additionally, the impact of recent episodes of intense rainfall has exacerbated soil erosion by further weakening the vegetation cover. These combined factors have led to the progressive deterioration of soil quality and an underestimation of the actual erosion risk in the model's outputs.

Table 6. Validation of the semi-quantitative model through comparison of predicted and observed erosion risk classes at control points (Developed by the authors)

Point n°	Name	X coordinate	Y coordinate	Observed class	Predicted class
1	Matatt	-7.943673	31.15729	Very low	Very low
2	Belghmime	-7.911589	31.17912	Very low	Very low
3	Tansghart	-7.965517	31.22618	Low	Low
4	Arghen	-7.921819	31.14389	Low	Low
5	Imsker	-7.938790	31.20410	Low	Low
6	Tagadirt	-7.981181	31.23108	Medium	Medium
7	Taddert	-7.922626	31.15149	Medium	Medium
8	Arg	-7.919683	31.18457	Medium	Medium
9	Moulay Brahim	-7.965458	31.28584	High	Very low
10	Imi Oughlad	-7.957374	31.20080	High	High
11	Imlil	-7.920757	31.13682	High	High
12	Al Aarb	-7.980004	31.24964	Very strong	High
13	Asselda	-7.970839	31.25060	Very strong	Very strong

Point n°	Name	X coordinate	Y coordinate	Observed class	Predicted class
14	Ait Souka	-7.911700	31.14025	Very strong	Very strong
15	Ouanesekra	-7.856835	31.15487	Very strong	Very strong

From the field observations, the total accuracy of the model was calculated using a multi-class confusion matrix (Table 7). After constructing the confusion matrix, five binary confusion matrices for each erosion risk class were derived. These binary matrices enabled the computation of classification metrics (Table 8) to evaluate the model's performance.

The metrics used for the analysis include:

$$*Accuracy = VP / (VP + FP)$$

$$*Recall = VP / (VP + FN)$$

$$*F1-score = (2 \times Accuracy \times Recall) / (Accuracy + Recall)$$

$$*Overall Accuracy = VP + VN / VP + FP + VN + FN$$

Where:

-True Positive (TP): The site belongs to the class and is correctly predicted.

-False Positive (FP): The site does not belong to the class, but the model predicts it as belonging to the class.

Table 7. Multi-class confusion matrix summarizing the comparison between predicted and actual erosion risk classes (Developed by the authors)

		Predicted Classes				
		Very Low	Low	Medium	High	Very Strong
Actual Classes	Very Low	2	0	0	0	0
	Low	0	3	0	0	0
	Medium	0	0	3	0	0
	High	1	0	0	2	0
	Very Strong	0	0	0	1	3

Table 8. Classification metrics for each erosion risk class based on the multi-class confusion matrix (Developed by the authors)

Class	Precision	Recall	F1-score
Very Low	0.66	1	0.79
Low	1.00	1	1.00
Medium	1.00	1	1.00
High	0.66	0.66	0.66
Very Strong	1.00	0.75	0.85

-True Negative (TN): The site does not belong to the class and is correctly predicted as such.

-False Negative (FN): The site belongs to the class, but the model predicts it as not belonging to the class.

-True Negative (TN): The site does not belong to the class and is correctly predicted as such.

-False Negative (FN): The site belongs to the class, but the model predicts it as not belonging to the class.

These metrics provide a comprehensive evaluation of the model's classification performance across all erosion risk classes.

These metrics provided valuable insights into the model's performance for each class. The very low, low, and medium classes were fully predicted by the model, while approximately two-thirds of the high-risk class and three-quarters of the very high-risk class were correctly predicted. The overall accuracy rate was estimated at approximately 86.67%, which confirms the reliability of the results and validates the model's effectiveness in estimating erosive risk.

6. Conclusion

The semi-quantitative assessment of gully erosion using the SCALES method, which incorporates both natural factors (such as slope, lithology, pedology, and land use) and social vulnerability factors (including population density, arboriculture, road networks, and socio-economic infrastructure), allowed for a comprehensive analysis and understanding of the gully erosion issue in the Rheraya watershed. The analysis classified the watershed into five categories of susceptibility, with medium and high-risk zones covering approximately half of the total area. This highlights a significant level of soil degradation, emphasizing the urgency of implementing targeted erosion control measures. The study also facilitated the creation of a multi-source geospatial database that can be continuously updated to monitor areas at risk and support informed land management decisions.

The results are consistent with previous research conducted in similar mountainous and semi-arid environments, which identified topography, lithology, and land use as dominant factors influencing gully development. However, the inclusion of socio-economic and infrastructural variables in the present study provides a more holistic assessment framework compared to earlier works, which often focused solely on physical factors. This integration underscores the importance of considering human vulnerability and land-use dynamics when evaluating erosion susceptibility.

From a theoretical standpoint, this study contributes to the advancement of semi-quantitative erosion modeling by demonstrating the applicability, efficiency, and adaptability of the SCALES method to complex mountainous environments such as the Western High Atlas. Practically, the findings offer decision-makers a rapid, cost-effective, and scalable tool for identifying

and prioritizing high-risk areas. The outcomes can support soil conservation planning, sustainable watershed management, and infrastructure protection within erosion-prone regions.

Future studies should aim to enhance the spatial resolution and accuracy of susceptibility mapping by incorporating higher-quality datasets, including time-series satellite imagery and detailed field observations. Validation of the model through on-site measurements would further strengthen its predictive reliability. Moreover, expanding the application of the SCALES approach to other watersheds in the Western High Atlas would facilitate regional-scale erosion risk assessment. Finally, integrating climate change scenarios and socio-economic development projections could provide valuable insights for designing long-term mitigation and adaptation strategies.

Acknowledgements

We would like to express our sincere gratitude to Professors Hassan Ibouh, Mohamed El Mehdi Saidi, Houcine Hannich, and Jalal Moustadraf, from the Faculty of Science and Technology at Cadi Ayyad University, Marrakech, for their generous sharing of knowledge and time. Their invaluable assistance with the technical aspects of the semi-quantitative model was crucial to the success of this study.

Declarations

Author contributions

Conceptualization, A.F. and F.E.W.; methodology, A.F., F.E.W.; software, A.F., F.E.W.; validation, A.F., F.E.W.; formal analysis, A.F., F.E.W.; investigation, A.F., F.E.W.; resources, A.F., F.E.W.; data curation, A.F., F.E.W.; writing—drafting the initial draft, A.F., F.E.W.; writing—revising and editing, A.F., F.E.W.; visualization, A.F., F.E.W.; supervision, A.F., F.E.W.; project administration, A.F., F.E.W.; funding acquisition, A.F., F.E.W.

All authors have read and approved the published version of the manuscript.

References

[1] DESTA, L. and ADUGNA, B. 2012. Nile Basin Initiative Eastern Nile Subsidiary Action Program (ENSAP) Eastern Nile Technical Regional Office (ENTRO) Eastern Nile Watershed Management Project A Field Guide on Gully Prevention and Control. www.nilebasin.org/entro.

[2] ROUET, I. 2009. Characterization and quantification of natural hazards linked to slope evolution in the ultrabasic massifs of New Caledonia. PhD thesis in applied geology, University of New Caledonia, France, 163p.

[3] FAO, 1990. Soil and water conservation in semi-arid zones. *Soil Bulletin*, vol. 57, p. 182.

[4] SABIR, M., MADDI, M., NAOURI, A., BARTHES, B. and ROOSE E. 2002. Runoff and Erosion Risks Indicators on the Main Soils of the Mediterranean Mountains of Occidental Rif Area (Morocco). 12th ISCO Conference, Beijing. Online: <https://topsoil.nserl.purdue.edu/isco/isco12/VolumeII/RunoffandErosionRisks.pdf>.

[5] NOUAIM, W., RAMBOURG, D., EL HARTI, A., ETTAQY, A., MERZOUKI, M. and KARAOUI, I. 2023. The estimation of water erosion with RUSLE and deposition model: A case study of the Bin El-Ouidane dam catchment area (High Atlas, Morocco). *Journal of Water and Land Development*, vol. 58 (VII-IX), pp. 136-147. DOI: [10.24425/jwld.2023.146606](https://doi.org/10.24425/jwld.2023.146606).

[6] AIT YACINE, E., OUDIJA, F., NASSIRI, L. and Essahlaoui, A. 2019. Modeling and Mapping of Soil Water Erosion Risks through the Application of GIS, Remote Sensing, and PAP/CAR Guidelines. Case Study of the Beht Watershed, Morocco. *European Scientific Journal*, vol.15, p. 259-285. DOI - [10.19044/esj.2019.v15n12p259](https://doi.org/10.19044/esj.2019.v15n12p259).

[7] ROOSE, E., SABIR, M. and LAOUINA, A. 2010. Sustainable water and soil management in Morocco: Promoting traditional Mediterranean techniques. IRD Éditions, Institut De Recherche Pour Le Développement, Marseille, pp. 15-30.

[8] MELIHO, M., KHATTABI, A., NOUIRA, A. and ORLANDO, C.A. 2021. Role of Agricultural Terraces in Flood and Soil Erosion Risks Control in the High Atlas Mountains of Morocco. *Earth*, vol. 2, p. 746-763. <https://doi.org/10.3390/earth2040044>.

[9] SAIDI, M. E. M., BOUKRIM, S., FNIGUIRE, F. and RAMROMI, A. 2012. Surface runoff in the High Atlas of Marrakech, Case of extreme debits. *Larhyss Journal*, n° 10, p. 75-90.

[10] HAJHOUI, Y. 2018. Rain-flow modeling and regime analysis of a semi-arid catchment under nival influence. Case of the Rhéraya catchment (High Atlas, Morocco). PhD thesis. Hydrology. Université Paul Sabatier - Toulouse III, France, 150p.

[11] CHAPONNIERE, A. 2005. Hydrological functioning of a semi-arid mountain watershed: case study of the Rhéraya watershed (Moroccan High Atlas). PhD, Institut National Agronomique, Paris.

[12] AHT GROUP and AG-RESING, 2016. Atlas of the Haouz-Mejjate Basin, Reraya Sub-basin. Atlas of the Haouz-Mejjate Basin, p. 122.

[13] LAMOUREUX, M. 1983. Fersiallitic soils. Garcia d'Orta, Sér. Est. Agron., Lisboa, vol. 10 (1-2), p. 11-18.

[14] LE GOUÉE, P., DELAHAYE, D., BERMOND, M., MARIE, M., DOUVINET, J. and VIEL, V. 2010. SCALES : a large-scale assessment model of soil erosion hazard in Basse-Normandie (northwestern

France). *Earth Surface Processes and Landforms*, vol. 35, n° 8, p. 887-901.

[15] CHEVALIER, P., HEBERT, A., KAUFMANT, Y. and MOYEN, J. 2001. Mapping the "soil erosion" hazard on Reunion Island: characterization and mapping of erosive phenomena. Report BRGM RP -51236-FR - 2001 SGR/REU 27. Saint-Denis: BRGM, 78 p.

[16] SOTI, V. 2003. Contribution of spatial remote sensing to the integrated management of the Saint-Gilles/La Saline lagoon on Reunion Island. An application example: mapping and monitoring of areas susceptible to soil erosion between 1995 and 2002 using Spot data integration. Montpellier: SILAT, Master's thesis, 39 p.

[17] SAATY, T.L. 1980. *The Analytic Hierarchy Process*. New York, USA, McGraw-Hill, 287, ISBN 0-07-054371-2.

[18] HENRY, J.B. 2006. Spatial information systems for flood risk management in lowlands. Doctoral thesis, University of Strasbourg I, France, 271p.

[19] BOU KHEIR, R., GIRARD, M.C., KHAWLIE, M. and ABADALLAH, C. 2001. Water erosion of soils in Mediterranean environments: a literature review. *Soil Study and Management*, vol. 8, no. 4, pp. 231-245.

[20] N'DRI, B.E., N'GO, Y.A., KADIO, H.N., OUATTARA, A., TOURÉ, B. and BIÉMI, J. 2008. Effect of soil slope and cover on runoff and rate of soil loss from experimental plots in the area of Attécoubé. *European Journal of Scientific Research*, vol. 21, n° 3, p. 459-470.

[21] RAMOS, S.C.E., GILBES, F., TORRES, P.D., RODRÍGUEZ, G.V. and ACEITUNO, J. 2014. Application of the Soil and Water Assessment Tool (SWAT) to estimate discharge and sediment yields from the Río Grande de Añasco Watershed, Puerto Rico. Unpublished report to the University of Puerto Rico-Sea Grant College Program.

[22] LUONG, A.T. 2012. Flood risk assessment in the Huong River basin, Thua Thien Hue province, central Vietnam. Thesis, Montreal (Quebec, Canada), University of Quebec in Montreal, Doctorate in Environmental Sciences.
<http://archipel.uqam.ca/id/eprint/4950>.

[23] BARA, F. 2012. Development of a geographic database for studying the vulnerability of Moroccan soils to water erosion in Morocco. Final thesis. National Forestry Engineering School, Salé, Morocco. 95 p.

[24] O'KEEFE, P., WESTGATE, K. and WESNER, B. 1976. Taking the naturalness out of natural disasters. *Nature*, vol. 260, p. 566-567.

参考文献

[1] DESTA, L. 和 ADUGNA, B. 2012. 尼罗河流域倡议东部尼罗河附属行动计划 (ENSAP) 东部尼罗河

技术区域办公室 (ENTRO) 东部尼罗河流域管理项目《沟蚀防治现场指南》。

www.nilebasin.org/entro.

[2] ROUET, I. 2009. 新喀里多尼亚超基性岩体斜坡演变相关自然灾害特征与量化研究. 应用地质学博士论文, 新喀里多尼亚大学, 法国, 163页.

[3] 联合国粮农组织, 1990.

《半干旱地区水土保持》。土壤公报, 第57卷, 第182页。

[4] SABIR, M., MADDI, M., NAOURI, A., BARTHES, B. 和 ROOSE E. 2002. 地中海西部里夫山区主要土壤径流与侵蚀风险指标 (摩洛哥)。第十二届国际水土保持大会, 北京。在线:

<https://topsoil.nserl.purdue.edu/isco/isco12/VolumeII/RunoffandErosionRisks.pdf>。

[5] 努艾姆, W.; 兰布尔, D.; 埃尔哈蒂,

A.; 埃塔基, A.; 梅尔祖基, M.; 卡拉乌伊, I.

2023. 基于RUSLE模型与沉积模型估算水蚀: 摩洛哥高阿特拉斯山脉宾埃尔乌伊丹水库集水区案例研究. 《水与土地开发杂志》, 第58卷 (VII-IX期), 第136-147页. DOI: 10.24425/jwld.2023.146606.

[6] AIT YACINE, E., OUDIJA, F., NASSIRI, L. 和 Essahlaoui, A. 2019. 基于GIS、遥感技术及PAP/CAR指南的土壤水蚀风险建模与制图: 摩洛哥贝赫特流域案例研究. 《欧洲科学期刊》第15卷, 第259-285页. DOI-10.19044/esj.2019.v15n12p259.

[7] ROOSE, E., SABIR, M. 和 LAOUINA, A. 2010. 《摩洛哥可持续水土管理: 推广传统地中海技术》。IRD出版社, 发展研究所, 马赛, 第15-30页。

[8] MELIHO, M., KHATTABI, A., NOUIRA, A. 和 ORLANDO, C.A. 2021. 梯田在摩洛哥高阿特拉斯山脉防洪防蚀中的作用. 《地球》第2卷, 第746-763页. <https://doi.org/10.3390/earth2040044>.

[9] SAIDI, M. E. M., BOUKRIM, S., FNIGUIRE, F. 和 RAMROMI, A. 2012. 马拉喀什高阿特拉斯山脉地表径流研究: 极端流量案例. 《Larhyss期刊》第10期, 第75-90页。

[10] HAJHOUI, Y. 2018. 受积雪影响的半干旱流域降雨-径流模型及水文过程分析: 以摩洛哥高阿特拉斯山脉雷拉亚流域为例. 博士学位论文. 水文学专业. 法国图卢兹第三大学保罗·萨巴蒂埃分校, 150页。

[11] CHAPONNIERE, A. 2005. 半干旱山区流域的水文功能: 以摩洛哥高阿特拉斯山脉雷拉亚流域为例. 博士学位论文, 巴黎国立农学研究院。

[12] AHT GROUP 与 AG-RESING, 2016. 《哈乌兹-梅贾特盆地图集: 雷拉亚次流域》。《哈乌兹-梅贾特盆地图集》, 第122页。

- [13] LAMOUREUX, M. 1983. 费尔西亚利特土壤。加西亚·德奥尔塔, 农业研究系列, 里斯本, 第10卷 (1-2期), 第11-18页。
- [14] LE GOUÉE, P., DELAHAYE, D., BERMOND, M., MARIE, M., DOUVINET, J. 和 VIEL, V. 2010. SCALES : 法国西北部下诺曼底地区土壤侵蚀风险的大尺度评估模型。《地表过程与地貌》, 第35卷, 第8期, 第887-901页。
- [15] CHEVALIER, P., HEBERT, A., 卡夫曼, Y. 与穆安, J. 2001. 《留尼汪岛土壤侵蚀风险图绘制: 侵蚀现象特征与制图》。报告BRGM RP-51236-FR-2001 SGR/REU 27。圣但尼: BRGM, 78页。
- [16] SOTI, V. 2003. 空间遥感技术对留尼汪岛圣吉尔/拉萨林泻湖综合管理的贡献。应用实例: 利用SPOT数据集集成技术对1995-2002年间易受土壤侵蚀区域进行制图与监测。蒙彼利埃: SILAT硕士学位论文, 39页。
- [17] SAATY, T.L. 1980. 《层次分析法》纽约, 美国, 麦格劳-希尔出版社, 287页, ISBN 0-07-054371-2。
- [18] HENRY, J.B. 2006. 低地洪水风险管理空间信息系统。博士论文, 法国斯特拉斯堡第一大学, 271页。
- [19] 布凯尔, R.; 吉拉尔, M.C.; 卡维, M.; 阿巴达拉, C. 2001. 地中海环境中的土壤水蚀: 文献综述。《土壤研究与管理》第8卷第4期, 第231-245页。
- [20] 恩德里, B.E.; 恩戈, Y.A.; 卡迪奥, H.N.; 瓦塔拉, A.; 图雷, B.; 比埃米, J. 2008. 土壤坡度与植被覆盖对阿特库贝地区试验地径流及土壤流失率的影响。《欧洲科学研究杂志》, 第21卷, 第3期, 第459-470页。
- [21] RAMOS, S.C.E., GILBES, F., TORRES, P.D., RODRÍGUEZ, G.V. 和 ACEITUNO, J. 2014. 土壤与水评估工具 (SWAT) 在波多黎各阿尼亚斯科大河流域径流与泥沙输沙量估算中的应用。提交波多黎各大学海洋赠款学院项目的未发表报告。
- [22] LUONG, A.T. 2012. 越南中部承天顺化省香河流域洪水风险评估。博士论文, 加拿大魁北克省蒙特利尔市, 魁北克大学蒙特利尔分校环境科学博士学位。 <http://archipel.uqam.ca/id/eprint/4950>。
- [23] 巴拉, F. 2012. 建立地理数据库以研究摩洛哥土壤对水蚀的脆弱性。毕业论文. 摩洛哥萨勒国立林业工程学院. 95页。
- [24] O'KEEFE, P., WESTGATE, K. 和 WESNER, B. 1976. 消除自然灾害的自然属性。《自然》杂志, 第260卷, 第566-567页。

Word count: 9,566 words, excluding references.

Peer-review record:

Fast-track status: Not fast-tracked

First-round reviews received: 3 reports

Revision cycles completed: 3 rounds

Final version submitted: October 6, 2025

Disclaimer/Publisher's Note:

The views, opinions and data expressed in this article are solely those of the authors and do not necessarily reflect those of the *Journal of Hunan University (Natural Sciences)* or its editors. The journal and its editorial staff accept no responsibility for any injury to persons or damage to property resulting from the ideas, methods, instructions or products discussed herein.